

1 Biogeochemical and plant trait mechanisms drive enhanced methane emissions
2 in response to whole-ecosystem warming

3
4 Genevieve L. Noyce and J. Patrick Megonigal

5 Smithsonian Environmental Research Center, Edgewater, MD

6
7 Corresponding author: G. Noyce, noyceg@si.edu, 443-482-2351

27 **Abstract**

28 Climate warming perturbs ecosystem carbon (C) cycling, causing both positive and negative
29 feedbacks on greenhouse gas emissions. In 2016, we began a tidal marsh field experiment in two
30 vegetation communities to investigate the mechanisms by which whole-ecosystem warming alters C gain,
31 via plant-driven sequestration in soils, and C loss, primarily via methane (CH₄) emissions. Here, we
32 report the results from the first four years. As expected, warming of 5.1 °C more than doubled CH₄
33 emissions in both plant communities. We propose this was caused by a combination of four mechanisms:
34 (i) a decrease in the proportion of CH₄ consumed by CH₄ oxidation, (ii) more C substrates available for
35 methanogenesis, (iii) reduced competition between methanogens and sulfate reducing bacteria, and (iv)
36 indirect effects of plant traits. Plots dominated by *Spartina patens* consistently emitted more CH₄ than
37 plots dominated by *Schoenoplectus americanus*, indicating key differences in the roles these common
38 wetland plants play in affecting anaerobic soil biogeochemistry and suggesting that plant composition can
39 modulate coastal wetland responses to climate change.

40

41 **1. Introduction**

42 Methane (CH₄) is a potent greenhouse gas that contributes to 15-19 % of total greenhouse gas
43 radiative forcing (IPCC, 2013) and has a sustained-flux global warming potential that is 45 times that of
44 CO₂ on a 100-year timescale (Neubauer & Megonigal, 2015). Wetlands are the largest natural source of
45 CH₄ to the atmosphere and were recently identified as the largest source of uncertainty in the global CH₄
46 budget (Saunois et al., 2016). Recent estimates calculate that CH₄ emissions from vegetated coastal
47 wetlands offset 3.6 of the 12.2 million metric tons (MMT) of CO₂ equivalents accumulated by these
48 ecosystems each year (EPA, 2017). Despite this, there is still a substantial knowledge gap regarding how
49 global change factors, such as climate warming, will alter coastal wetland CH₄ emissions (Mcleod et al.,
50 2011) even though these feedbacks have the potential to shift coastal wetlands from being a net sink of C
51 to a net source (Al-Haj & Fulweiler, 2020; Bridgman et al., 2006).

52 The net flux of CH₄ to the atmosphere from any ecosystem represents the balance between the
53 amount of CH₄ produced (methanogenesis), the amount of CH₄ oxidized (methanotrophy), and the rate of
54 CH₄ transport from the soil. Rates of methanogenesis are driven by low redox conditions and substrate
55 availability, while aerobic CH₄ oxidation requires both O₂ and CH₄ as substrates. Roots and rhizomes in
56 wetland ecosystems influence methane-related substrates through at least two mechanisms: (i) deposition
57 of organic compounds that support multiple pathways of heterotrophic microbial respiration, including
58 methanogenesis, and (ii) release of O₂ that simultaneously promotes CH₄ oxidation (Philippot et al., 2009;
59 Stanley & Ward, 2010) and regeneration of competing electron acceptors such as Fe(III) and SO₄²⁻. Root
60 exudates, which typically include low-molecular-weight compounds, may either be more readily used by microbes than
61 existing soil C (Kayranli et al., 2010; Megonigal et al., 1999) (Kayranli et al., 2010; Megonigal et al.,
62 1999) or may prime microbial use of soil C (Basiliko et al., 2012; Philippot et al., 2009; Robroek et al.,
63 2016; Waldo et al., 2019) (Basiliko et al., 2012; Philippot et al., 2009; Robroek et al., 2016; Waldo et al.,
64 2019). Root exudates can also decrease CH₄ oxidation by stimulating use of O₂ by other aerobic microbes
65 (Lenzewski et al., 2018; Mueller et al., 2016). Consequently, wetland CH₄ emissions are strongly linked
66 to soil C quality and quantity. The following sections will describe the processes that control CH₄ production
67 and oxidation in wetland ecosystems, and how these processes are influenced by soil C quality and quantity.
68

77 to a wide variety of plant traits that govern the supply of reductive (organic carbon) and oxidative (O_2)
78 substrates to soils (Moor et al., 2017; Mueller et al., [in press](#)2020).

Field Code Changed

79 Although it is understood that wetland plants are a primary control on CH_4 emissions and that much
80 of their influence is mediated through conditions in the rhizosphere (Waldo et al., 2019), there are
81 surprisingly few data, especially from coastal wetlands, that couple plant responses to the dynamics of
82 electron donors (organic C), electron acceptors (O_2 , SO_4), and the rates of competing (sulfate reduction vs
83 methanogenesis) or opposing (CH_4 production vs CH_4 oxidation) microbial processes. The general lack of
84 process data on wetland CH_4 cycling makes it difficult to forecast ecosystem responses to climate change.
85 For example, the well-documented observation that warming increases wetland methane emissions can be
86 either amplified or dampened depending on changes in plant activity (e.g. primary production) or plant
87 traits (e.g. community composition) (Mueller et al., [in press](#))(Mueller et al., 2020). Vegetation
88 composition has been shown to be a stronger control on CH_4 emissions than ~ 1 °C of warming in
89 northern peatlands (Ward et al., 2013) and Chen et al. (2017)Chen et al. (2017) proposed that warming
90 effects on plant functional types can drive C flux responses that cannot otherwise be explained by abiotic
91 conditions. In freshwater marshes, plant species and growth trends have also been linked to seasonal
92 shifts in pools of dissolved CH_4 and DIC (Ding et al., 2005; Stanley & Ward, 2010)(Ding et al., 2005;
93 Stanley & Ward, 2010) and methanogenesis dynamics (Sorrell et al., 1997)(Sorrell et al., 1997).

94 Tidal wetlands are particularly good model systems for determining the mechanisms by which
95 warming alters CH_4 emissions. Not only will the CH_4 cycle respond to the direct effects of warming, but
96 the temperature effects on the outcome of competition for electron acceptors is relatively easily observed
97 because of the abundance of SO_4 . Thermodynamic theory in which terminal electron acceptors (TEAs)
98 are used in order of decreasing thermodynamic yield is commonly interpreted to mean that a system will
99 support only one form of anaerobic respiration at time, with methanogenesis occurring only when pools
100 of more energetically favorable TEAs have been depletedacetoclastic and hydrogenotrophic
101 methanogenesis occurring only when pools of more energetically favorable TEAs have been depleted
102 (Conrad, 2020; Schlesinger & Bernhardt, 2020). However, in real systems with spatial and temporal

103 variability in the supply of electron donor substrates and TEAs, all forms of anaerobic metabolism occur
104 simultaneously (Megonigal et al. 2004, Bridgman et al., 2013). Much of this spatial and temporal
105 variation arises from the distribution and activity of roots and rhizomes as mediated by the rhizosphere
106 (Neubauer et al., 2008). Global change factors such as warming will further affect the spatial distribution
107 of key metabolic substrates. In addition, the relatively ~~limited~~ species diversity in saline tidal wetlands
108 allows species-level effects on CH₄ cycling to be delineated more easily than in diverse freshwater
109 wetlands.

110 Methane flux measurements are a metric of broader shifts in redox potential and biogeochemical
111 cycling, as they are sensitive to virtually all processes that regulate availability of electron donors and
112 electron acceptors. Emissions are commonly predicted to increase with future climate warming, including
113 from coastal wetlands (Al-Haj & Fulweiler, 2020), but there is minimal prior understanding of the
114 underlying mechanisms, which was the focus of this study. Our objectives were to explore the
115 mechanisms that drive enhanced CH₄ emissions under warming. To accomplish this, we measured
116 monthly CH₄ emissions from 2016 through 2019 and coupled these flux measurements with analysis of
117 porewater biogeochemistry and vegetation biomass and composition.

118

119 **2. Materials and Methods**

120 2.1 Site Description and Experimental Design

121 The Salt Marsh Accretion Response to Temperature eXperiment (SMARTX) was established in the
122 Smithsonian's Global Change Research Wetland (GCReW) in 2016. GCReW is part of Kirkpatrick
123 Marsh, a microtidal, brackish high marsh on the western shore of the Chesapeake Bay, USA (38°53' N,
124 76°33' W). Soils are organic (>80 % organic matter) to a depth of 5 m, which is typical of high marshes
125 in the Chesapeake Bay. ~~The marsh is typically saturated to within 5-15 cm of the soil surface, but~~
126 ~~inundation frequency varies across the site, from 10-20 % of high tides in high elevation areas to 30-60 %~~
127 ~~of and elsewhere. The very low mineral content (<20%) affects methane dynamics because negligible~~
128 ~~competition between methanogens and iron-reducing bacteria for electron donors is expected in the~~

129 absence of a significant pool poorly crystalline iron oxides (Roden & Wetzel, 1996), as has been
130 documented previously at this site (Weiss et al., 2004) (Weiss et al. 2004). Soil bulk density in the upper
131 60 cm averages 0.124 g cm³ and ranges from 0.079 to 0.180 g cm³. The relatively uniform bulk density of
132 the soil profile reflects the uniform soil organic matter content and the fact that bulk density becomes
133 largely independent of organic matter and mineral content once organic matter content exceeds 50%
134 (Holmquist et al., 2018). The marsh is typically saturated to within 5-15 cm of the soil surface, but
135 inundation frequency varies across the site, from 10-20 % of high tides in high elevation areas to 30-60 %
136 of high tides in low elevation areas.

137 SMARTX consists of six replicate transects, three located in each of the two dominant annual plant
138 communities (Fig. S1). In the C₃-dominated community (herein the ‘C₃ community’) the C₃ sedge
139 *Schoenoplectus americanus* (herein *Schoenoplectus*) composes more than 90 % of the aboveground
140 biomass (Table 1). In the C₄-dominated community (herein the ‘C₄ community’), 75 % of the
141 aboveground biomass was initially composed of two C₄ grasses (*Spartina patens* and *Distichlis spicata*,
142 herein *Spartina* and *Distichlis*, respectively). However, by 2019, *Spartina* and *Distichlis* declined to 56 %
143 of the aboveground biomass (Table 1).

Table 1. Relative contribution to total aboveground biomass from C₃ sedges (*Schoenoplectus americanus*) and C₄ grasses (*Spartina patens* and *Distichlis spicata*) in each plant community. Values are means and SE (n = 12).

Year	C ₃ community		C ₄ community	
	% C ₃	% C ₄	% C ₃	% C ₄
2016	93 (3)	8 (3)	8 (2)	76 (6)
2017	91 (3)	9 (3)	10 (3)	64 (4)
2018	95 (1)	5 (1)	15 (4)	65 (7)
2019	93 (2)	4 (1)	23 (5)	56 (6)

144 Each transect is an active warming gradient consisting of unheated ambient plots and plots that
145 are heated to 1.7 °C, 3.4 °C, and 5.1 °C above ambient. All plots are 2 x 2 meters with a 20 cm-wide
146 buffer around the perimeter. Aboveground plant-surface temperature is elevated via infrared heaters and
147 soil temperature is elevated via vertical resistance cables (Rich et al., 2015)(Rich et al., 2015). Soils are
148 heated to a depth of 1.5 m, which is the depth most vulnerable to climate or human disturbance
149 (Pendleton et al., 2012). Aboveground and belowground temperature variation are assessed via

150 thermocouples embedded in acrylic plates at plant canopy level and inserted into the soil, respectively,
151 and the temperature gradient is maintained by integrated microprocessor-based feedback control (Rich et
152 al., 2015). Aboveground and belowground temperature variation are assessed via thermocouples embedded
153 in acrylic plates at plant canopy level and inserted into the soil, respectively, and the temperature gradient
154 is maintained by integrated microprocessor-based feedback control (Rich et al., 2015). Noyce et al. (2019)
155 provides additional details of the heating system. Warming began on 1 Jun 2016 and has continued year-
156 round.

157 2.2 Methane flux measurements

158 Methane emissions were measured monthly year-round from May 2016 to Dec 2019 using a static
159 chamber system. One permanent 160 cm² aluminum base was inserted 10 cm into the soil in each plot in
160 Apr 2016. On each measurement date, clear chambers (40 x 40 x 40 cm) were gently placed on top of
161 each base and secured with compression clips. Chambers consisted of an aluminum frame with
162 transparent sides made of polychlorotrifluoroethylene film (Honeywell International) and closed-cell
163 foam on the base. Depending on the height of the vegetation at the time of measurement, chambers were
164 stacked up to four high (total height of 40 to 160 cm) (Fig. S2). The advantage of this stacking method is
165 that it uses the minimal chamber volume necessary, while also allowing for plant growth. After
166 placement, the chambers were left open for at least 10 minutes, to minimize disturbance effects and allow
167 air inside the chamber to return to ambient conditions. During data collection, chambers were covered
168 with a transparent polycarbonate top equipped with sampling tubes, a fan to circulate air inside the
169 chambers, a PAR sensor, and thermocouples. The sealed chamber was covered with a foil shroud to block
170 out all light and to minimize changes in temperature and relative humidity during the measurement
171 period. An UltraPortable Greenhouse Gas Analyzer (Los Gatos Research, CA) was used to measure
172 headspace CH₄ concentrations for 5 min. Plots were accessed from permanent boardwalks elevated 15 cm
173 above the soil surface to avoid compressing the surrounding peat and altering diffusive CH₄ emissions.
174 Fluxes were calculated as the slope of the linear regression of CH₄ concentration over time. The 40 fluxes
175 where $p > 0.05$ were assigned a value of $\frac{1}{2}$ the limit of detection of the system (Wassmann et al., 2018;

176 Table S1). This was 1 % of fluxes during the growing season and 4.5 % of fluxes over the remaining
177 months. For 2017-2019, monthly measurements were scaled to annual estimates by regressing CH₄
178 emissions against daily mean soil temperature and day of year (as a proxy for phenological status).
179 Annual estimates were not calculated for 2016 because flux measurements did not start until May.

180 2.3 Porewater sampling and analysis

181 Porewater samples were collected in May, Jul, and Sep of each year using stainless steel 'sippers'
182 permanently installed in each plot. Each sipper consisted of a length of stainless-steel tubing, crimped and
183 sealed at the end, with several slits (approximate width 0.8 mm) cut in the bottom 2 cm. The aboveground
184 portion of each sipper was connected to Tygon Masterflex® tubing capped with a 2-way stopcock. In
185 May 2016, duplicate clusters of sippers were installed in each of the 30 plots at 20, 40, 80, and 120 cm
186 below the soil surface. An additional set of 10 cm-deep sippers was installed in 2017. In this study we
187 defined samples from 10-20 cm as "rooting zone" samples and samples from 40-120 cm as "deep peat"
188 samples. On sampling dates, porewater sitting in the sippers was drawn up and discarded, after which 60
189 mL of porewater from each depth (30 mL from each sipper) was withdrawn and stored in syringes
190 equipped with 3-way stopcocks. A 10 mL-aliquot of each sample was filtered through a pre-leached 0.45
191 µm syringe-mounted filter, preserved with 5 % zinc acetate and sodium hydroxide, and frozen for future
192 SO₄ and Cl analysis. Dissolved CH₄ was extracted from 15 mL of porewater in the syringe by drawing 15
193 mL of ambient air and shaking vigorously for 2 min to allow the dissolved CH₄ to equilibrate with the
194 headspace. Headspace subsamples were then immediately analyzed on a Shimadzu GC-14A gas
195 chromatograph equipped with a flame ionization detector. 3 mL of porewater was used to measure pH
196 using a Fisher Scientific accumet electrode (13-620-290). The remaining porewater was used to measure
197 pH, H₂S, and NH₄; those data are not reported here.

198 SO₄ and Cl were measured on a Dionex ICS-2000 ion chromatography system (2016-2018) or a
199 Dionex Integrion (2019). On the Dionex ICS-2000 samples were separated using an AA11A11 column
200 with 30 mM of KOH as eluent; on the Dionex Integrion samples were separated using an AA11A11-
201 4µm-fast column with 35 mM KOH. Sulfate depletion (Sulfate_{Dep}) was calculated based on measured

202 porewater concentrations of SO_4 (SO_4_{pw}) and Cl (Cl_{pw}) and the constant molar ratio of Cl to SO_4 in
203 surface seawater ($R_{\text{sw}} = 19.33$; [Bianchi 2006](#)) using the following equation: $\text{Sulfate}_{\text{Dep}} = \text{Cl}_{\text{pw}} / R_{\text{sw}} - \text{SO}_4_{\text{pw}}$.
204 [Based only on Bianchi, 2006](#) using the following equation: $\text{Sulfate}_{\text{Dep}} = \text{Cl}_{\text{pw}} / R_{\text{sw}} - \text{SO}_4_{\text{pw}}$. If driven only
205 by seawater inputs, the ratio of Cl to SO_4 would remain constant, but under anaerobic conditions SO_4 can
206 be reduced by sulfate reducing bacteria, altering this ratio. As a result, SO_4 depletion can be used as a
207 proxy for SO_4 reduction rates.

208 2.4 Plant biomass measurements

209 Measurements of *Schoenoplectus*, *Spartina*, and *Distichlis* biomass were conducted during peak
210 biomass of each year (29 Jul – 2 Aug) as described by Noyce et al. (2019). *Schoenoplectus* biomass was
211 estimated using non-destructive allometric techniques (Lu et al., 2016) in 900-cm² quadrats, and *Spartina*
212 and *Distichlis* biomass were estimated through destructive harvest of 25-cm² subplots.

213 2.5 Data analysis

214 Statistics were conducted in R (version 3.6.3). [ANOVA tests were used to compare means between](#)
215 [warming treatments and plant communities, with Tukey's HSD test for post hoc analyses. The 'growing](#)
216 [season' was defined as May through Sep, based on *Schoenoplectus* growth trends \(see Fig. S3\). Due to](#)
217 [the non-normal distribution of the \$\text{CH}_4\$ flux \(Fig. S4\) and porewater data, values were log transformed](#)
218 [prior to calculating Methane flux \(Fig. S3\) and porewater data were log transformed to become normally](#)
219 [distributed prior to statistical analyses. The 'growing season' was defined as May through Sep based on](#)
220 [Schoenoplectus growth trends \(Fig. S4\). Pearson's correlations were used to test the relationships](#)
221 [between \$\text{CH}_4\$ flux and soil temperature, and \$\text{CH}_4\$ flux and plant biomass. Responses of \$\text{CH}_4\$ emissions to](#)
222 [vegetation type and warming treatment were analyzed using linear mixed models with vegetation](#)
223 [community and warming treatment as categorial variables, and plot and year as random effects. P-values](#)
224 [were calculated using Satterthwaite's method and Tukey's post-hoc tests were used to compare](#)
225 [individual means. Porewater data was averaged per year and then analyzed using one-way ANOVAs to](#)
226 [determine the effects of warming treatment or plant community, applying Tukey's HSD test for post-hoc](#)
227 analyses.

228

229 **3. Results**230 3.1 Environmental conditions, site characteristics, and experiment performance

231 The growing season of 2016 was the hottest of the four years, with growing season temperatures
 232 averaging >1 °C above the other three years (Table 2). While 2017 through 2019 had similar summer
 233 temperatures, they had very different precipitation regimes; 2018 was much wetter on average and 2019
 234 was slightly drier (Table 2). During all years, temperatures in the experimental plots were successfully
 235 shifted by the target differentials of +1.7, +3.4, and +5.1 °C above the ambient plots (Fig. 1; Noyce et al.,

236 2019). Porewater pH ranged from 6.4 to 6.8 across the measurement period, with no effect of temperature

237 treatment ($p > 0.1$; data not

Year	Mean aboveground temperature (°C)	Mean soil temperature (°C)	Total precipitation (cm)
2016	24.7 (0.3)	22.4 (0.2)	51.0
2017	22.0 (0.3)	20.7 (0.2)	51.1
2018	23.7 (0.3)	20.8 (0.2)	86.4
2019	23.6 (0.3)	20.9 (0.2)	43.7

241 ambient and +5.1 °C plots after 4.5 years of warming ($p = 0.54$; data not shown).

242

Table 2. Growing season (May-Sep) temperature and precipitation. Temperature data are means (SE) of daily averages from ambient plots and precipitation is total from May through September.

Year	Mean aboveground temperature (°C)	Mean soil temperature (°C)	Total precipitation (cm)
2016	24.7 (0.3)	22.4 (0.2)	51.0
2017	22.0 (0.3)	20.7 (0.2)	51.1
2018	23.7 (0.3)	20.8 (0.2)	86.4
2019	23.6 (0.3)	20.9 (0.2)	43.7

243 3.2 Methane fluxes

244 Methane emissions increased with soil temperature ($R^2 = 0.41$, $p < 0.001$) (Fig. 1). Emissions from
 245 all treatments had strong seasonal trends; fluxes were highest in the C₃ community in Jun through Aug
 246 and peak fluxes in the C₄ community were shifted about a month later to Jul through Sep (Fig. S4S3).
 247 Whole-ecosystem warming increased CH₄ emissions throughout the growing season ($F_{3,430} = 3.7_{400} = 5.1$,

248 $p = 0.012002$; Fig. 2). Across all four years, $5.1\text{ }^{\circ}\text{C}$ of warming more than doubled growing season
 249 emissions, from 624 to $1413\text{ }\mu\text{mol CH}_4\text{ m}^{-2}\text{ d}$ ($p_{\text{adj}} = 0.0402$; Fig. 2).

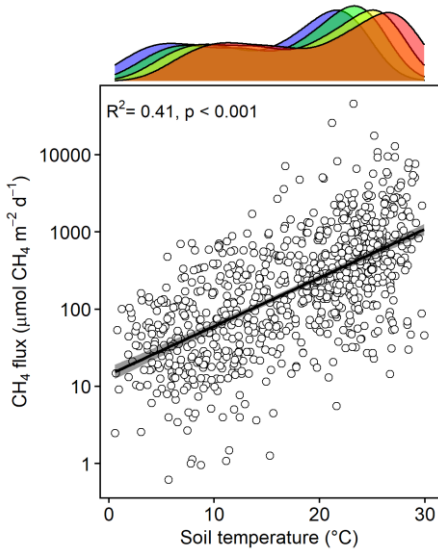


Figure 1. CH_4 emissions from each plot versus the soil temperature at the time of measurement. Density plot shows the range of soil temperatures in each treatment.

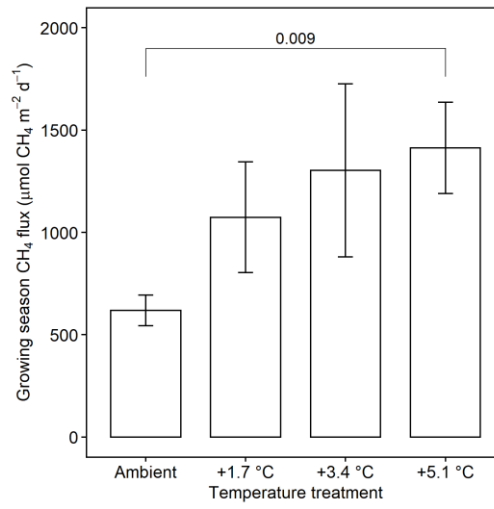
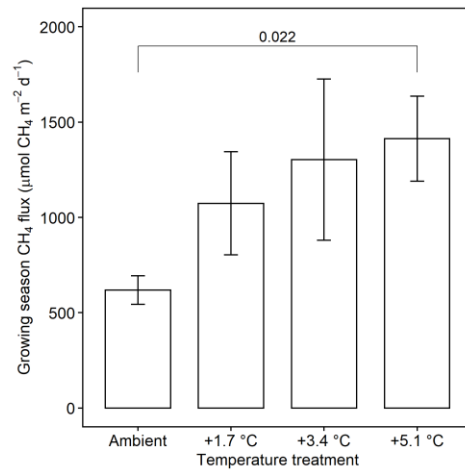


Figure 2. Comparison of CH_4 emissions from each warming treatment during the growing season (May-Sep). Means include both the C_3 and C_4 community and all years of measurement. Error bars indicate SE. Horizontal bars indicate means that are significantly different and the corresponding p_{adj} .

250
 251
 252 Mean CH₄ emissions were higher from the C₄
 253 community than from the C₃ community both
 254 during the growing season ($F_{1,20} = 22.0, p = 13.6$, p
 255 ≤ 0.001 ; Fig. 3a) and on an annual basis ($F_{1,20} = 10.2, p = 8.5$, $p = 0.002008$; Fig. 3b). Mean
 256 annual CH₄ emissions ranged from 58 mmol
 257 CH₄ m⁻² yr⁻¹ (ambient) to 343 mmol CH₄ m⁻² yr⁻¹
 258 (+5.1 °C) in the C₃ community and from 55
 259 (+5.1 °C) in the C₃ community and from 55



260 Figure 1. Bottom: CH₄ emissions from each plot
 261 versus the soil temperature at the time of
 262 measurement. Top: Density plot depicting the
 263 range of soil temperatures in each treatment.

mmol CH₄ m⁻² yr⁻¹ (ambient) to 879 mmol CH₄ m⁻² yr⁻¹
 (+5.1 °C) in the C₄ community (Table S2). Under
 ambient conditions, growing season CH₄ fluxes were
 almost twice as large from C₄ plots, whereas under low

264 warming (1.7-to 3.4 °C) this difference increased to more than three times as large (Fig. 3a). From 2017-
 265 2019, CH₄ emissions were positively related to *Spartina* and *Distichlis* aboveground biomass across all
 266 warming treatments and negatively related to *Schoenoplectus* biomass (Fig. 4a,b). In 2016, however, the
 267 direction of those relationships in both plant communities were the exact opposite, with *Spartina* and

268 *Distichlis* biomass negatively related, and *Schoenoplectus* biomass positively related, to CH₄ emissions

269 (Fig. 4a,b).

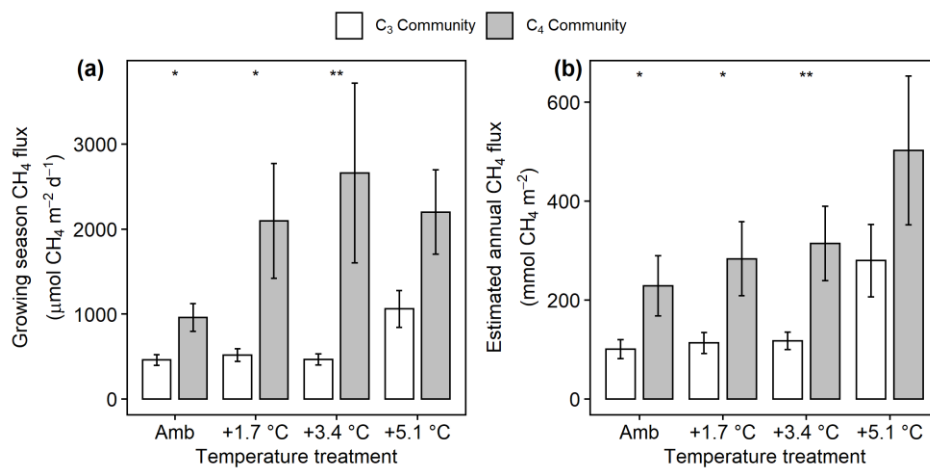


Figure 3. Comparison of CH₄ emissions from the C₃ community dominated by *Schoenoplectus* (open bars) and the C₄ community dominated by *Spartina* and *Distichlis* (grey bars). (a) During the growing season (May–Sep) and (b) scaled to a year. Means are averaged across all sampling dates for 2017–2019. Error bars indicate SE. Asterisks indicate significant differences between C₃ and C₄ means at a given temperature (* p_{adj} < 0.05, ** p_{adj} < 0.01).

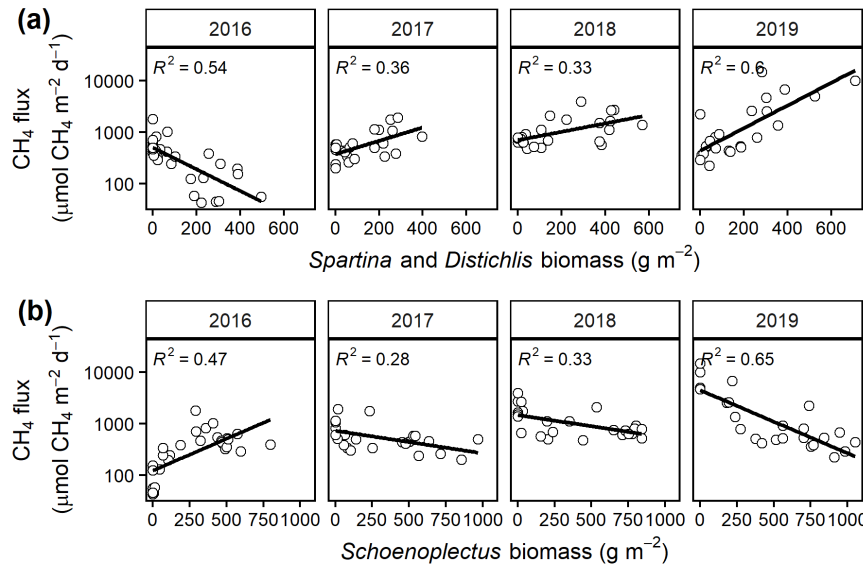


Figure 4. Mean growing season (May–Sep) CH₄ emissions from each plot versus the biomass of (a) C₃ (*Schoenoplectus*) and (b) C₄ (*Spartina* and *Distichlis*) plants. All regressions are significant at $p = 0.05$.

270 3.3 Porewater chemistry

271 Under ambient conditions, porewater collected from the C₄ community had lower salinity ($F_{1,315} = 15.5, p < 0.001$), more dissolved CH₄ ($F_{1,315} = 45.0, p < 0.001$; Fig. 5a,b), and less SO₄ ($F_{1,315} = 61.5, p < 0.001$; Fig. 6a) than, and similar salinity ($p = 0.068$) compared to the C₃ community. In 272 the C₃ community, warming increased dissolved CH₄ in both the rooting zone porewater (i.e. 10–20 cm) 273 ($F_{3,225} = 5.45, p = 0.001048$; Fig. 5a) and in the deep peat (40–120 cm) ($F_{3,366} = 13.44, p = 0.00000623, p \leq 274 0.001$; Fig. 5b). Dissolved CH₄ concentrations were relatively similar in the ambient, +1.7 °C, and +3.4 275 °C treatments, but more than doubled with +5.1 °C of warming in both the rooting zone (59 to 125 μmol 276 CH₄ L⁻¹, $p_{adj} \leq 0.001$) and the deeper porewater (43 to 1254 μmol CH₄ L⁻¹, $p_{adj} < 0.001$). In the C₄ 277 community there was minimal effect of warming treatment on porewater in the rooting zone ($F_{3,230} = 5.45, p = 0.0442, p = 0.6772$; Fig. 5a), but all levels of warming decreased dissolved CH₄ below 40 cm 278 279 280

281 (F_{3,379} = 39.44, $p < 0.001$), with concentrations in the +3.4 and +5.1 plots less than a third of the
 282 concentrations in the ambient plots (155 vs 56 and 40 $\mu\text{mol CH}_4 \text{ L}^{-1}$, $p_{\text{adj}} < 0.001$; Fig. 5b).

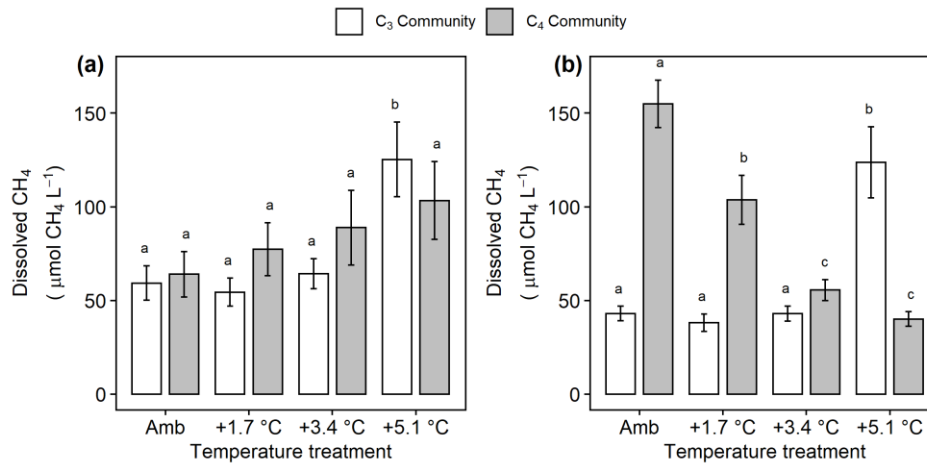


Figure 5. Comparison of dissolved CH_4 from the C_3 community dominated by *Schoenoplectus* (open bars) and the C_4 community dominated by *Spartina* and *Distichlis* (grey bars). (a) In the dominant rooting zone (10–20 cm) and (b) below the rooting zone (40–120 cm). Means are averaged across all sampling dates for 2016–2019. Error bars indicate SE. Letters indicate temperature treatments that are significantly different from each other ($p_{\text{adj}} < 0.05$) within the same plant community.

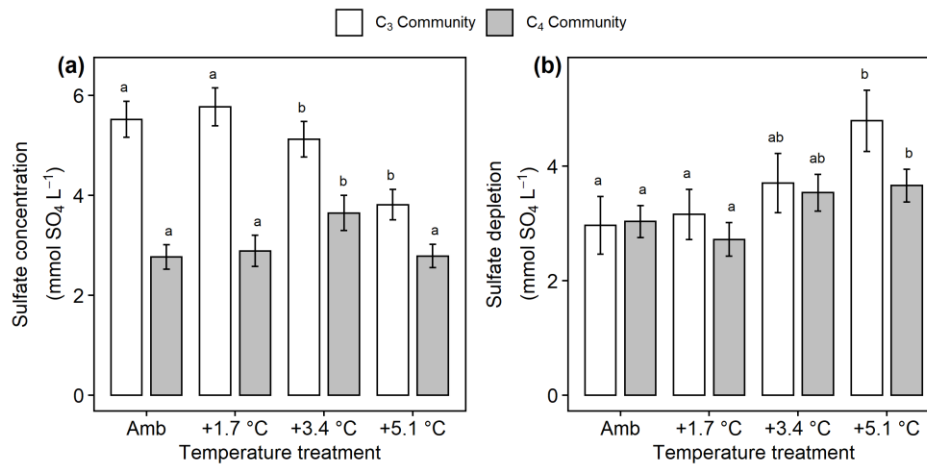


Figure 6. Comparison of sulfate concentrations and estimated sulfate depletion from the C_3 community dominated by *Schoenoplectus* (open bars) and the C_4 community dominated by *Spartina* and *Distichlis* (grey bars). (a) Sulfate concentration and (b) sulfate depletion in the rooting zone. Means are averaged across all sampling dates for 2016–2019. Error bars indicate SE. Letters indicate temperature treatments that are significantly different from each other ($p_{\text{adj}} < 0.05$) within the same plant community.

across all sampling dates for 2016 – 2019. Error bars indicate SE. Letters indicate temperature treatments that are significant different from each other ($p_{adj} < 0.05$) within the same plant community.

283 In the C₃ community, warming of +3.4 and +5.1 °C reduced SO₄ concentrations decreased with
284 warming (F_{3,597} = 11.7₄₄ = 3.76, $p \leq 0.004017$), but warming effects on SO₄ cycling in the C₄ community
285 were more mixed with +3.4 °C increasing SO₄ ($p_{adj} = 0.013048$) but no other treatments having large
286 effects (Fig. 6a). In all plots, the measured concentrations of rooting-zone SO₄ were lower than expected
287 based on salinity (Fig. 6b), indicating that SO₄ reduction occurred. In both plant communities, the +5.1 °C
288 treatments increased this SO₄-depletion effect compared to ambient (though the effect was stronger in
289 the C₃: F_{3,340} = 3.96, community ($p \leq 0.008$; C₄: F_{3,258} = 3.04, 0.01) than the C₄ community ($p =$
290 0.029)04). (Fig. 6b). In Dissolved CH₄ was highest in both plant communities, dissolved CH₄ was highest
291 when SO₄ concentrations were below 5 mmol SO₄ L⁻¹ (Fig. S5).

292

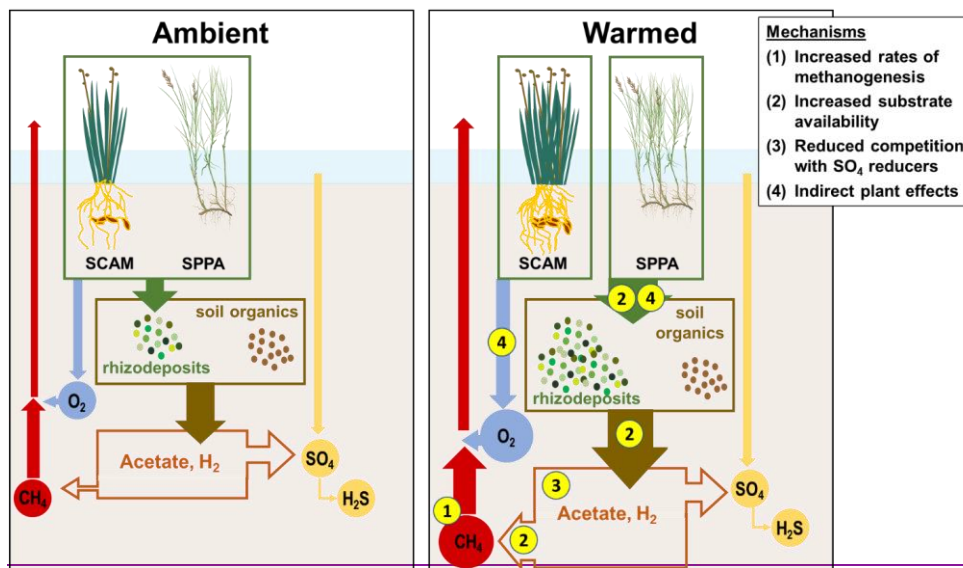
293 4. Discussion

294 Soil temperature (both seasonal and experimental) and plant traits were both strong drivers of CH₄
295 emissions from this site. This follows prior field, mesocosm, and incubation studies across a variety of
296 wetlands, in which temperature has been shown to be a strong predictor of CH₄ emissions (e.g. Al-Haj
297 and Fulweiler, 2020; van Bodegom and Stams, 1999; Christensen et al., 2003; Dise et al., 1993; Fey and
298 Conrad, 2000; Liu et al., 2019; Ward et al., 2013; Yang et al., 2019; Yvon-Durocher et al., 2014) Al-Haj
299 and Fulweiler, 2020; van Bodegom and Stams, 1999; Christensen et al., 2003; Dise et al., 1993; Fey and
300 Conrad, 2000; Liu et al., 2019; Ward et al., 2013; Yang et al., 2019; Yvon-Durocher et al., 2014) and in
301 which plant functional type has an interacting effect (e.g. Chen et al., 2017; Duval & Radu, 2018; Liu
302 et al., 2019; Mueller et al., in press 2020; Ward et al., 2013). Methane emissions are a function of the
303 balance between methanogenesis, CH₄ oxidation, and CH₄ transport, so explaining these results requires
304 some combination of stimulation of methanogenesis, reduction of CH₄ oxidation, or increase in CH₄
305 transport.

306 Prior data from brackish wetlands are limited, but incubation studies on freshwater wetland soils
307 typically show large increases in CH₄ fluxes with warming (Duval & Radu, 2018; Hopple et al., 2020;
308 Inglett et al., 2012; Sihi et al., 2017; van Bodegom & Stams, 1999; Wilson et al., 2016), indicating that

Field Code Changed

309 warming alters belowground processes. Though there is some evidence that rhizosphere temperature
 310 alters CH_4 transport through rice aerenchyma (Hosono & Nouchi, 1997), any transport-driven effects in
 311 this ecosystem would be transient unless there was a simultaneous increase in net CH_4 production (i.e. an
 312 increase in methanogenesis that was not completely offset by methanotrophy). Instead, we observed a
 313 sustained increase in CH_4 emissions, suggesting large shifts in anaerobic metabolism, especially with +5.1
 314 °C of warming. We propose four potential and non-exclusive mechanisms to explain the temperature-
 315 driven increase in CH_4 emissions: (1) shifted ratios of CH_4 production to oxidation, (2) increased substrate
 316 availability, (3) reduced competition with sulfate reducers for H_2 and organic C, and (4) indirect plant trait
 317 effects (Fig. 7).



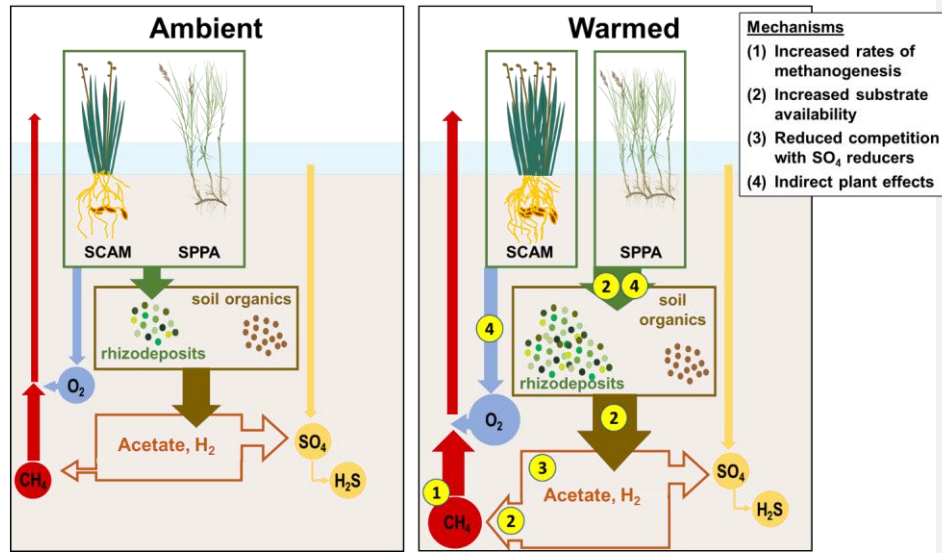


Figure 7. Schematic of mechanisms driving enhanced CH_4 emissions in response to warming. SCAM = *Schoenoplectus americanus*. SPPA = *Spartina patens*. Left: Processes under ambient conditions. Plants add organic compounds to the soil, which are transformed into other low-molecular-weight organic compounds. This pool, and processed soil organic matter, support terminal respiration processes dominated by SO_4 reduction over CH_4 production in organic-rich brackish marsh soils. Plants also transport O_2 which supports oxidation of a fraction of the CH_4 before it can be transported out of the soil. Right: Processes under warmed conditions. 1) Rates of CH_4 production increase more than rates of CH_4 oxidation. 2) Substrate availability increases as plants add more rhizodeposits and organic matter is more rapidly fermented to low-molecular-weight organic compounds and H_2 . 3) The pool of electron donors available to methanogens increases as SO_4 reducers become SO_4 limited. 4) The dominant plant species have different effects on these process with *S. americanus* driving a net increase in O_2 transport and *S. patens* driving a net increase in rhizodeposits.

319 4.1 Whole-ecosystem warming promotes methanogenesis over CH_4 oxidation

320 Holding the supply of substrates and transport properties of the system constant, warming is expected
 321 to increase rates of CH_4 production relative to CH_4 oxidation due solely to differences in the temperature
 322 dependence of each process (Megonigal et al., 2016). In wetland soils, the
 323 average Q_{10} of methanogenesis is 4.1 compared to 1.9 for aerobic CH_4 oxidation (Segers, 1998), which means that a system starting with a given initial ratio between the two processes will
 324 become increasingly dominated by methanogenesis as soils warm. A corollary to this expected pattern is
 325 that the ratio of the two processes should be constant if the Q_{10} responses are similar, an outcome that was
 326 supported with *in situ* measurements of the two

328 processes in a tidal freshwater forested wetland (Megonigal & Schlesinger, 2002). We did not quantify
329 the temperature dependence of CH₄ production and oxidation in the present study, but based on the
330 literature (Segers, 1998) it is likely that methanogenic activity increased more than aerobic
331 methanotrophic activity in direct response to warming (Fig. 7, mechanism 1). Evidence for this is that
332 rhizosphere pools of porewater CH₄ were highest in the warmest treatment (Fig. 5a); because this
333 occurred despite either no change or an increase in aboveground biomass (Noyce et al., 2019) which
334 would by itself have lowered porewater CH₄ due to venting (plant transport), it indicates that CH₄
335 production increased relative to the sum of aerobic and anaerobic methane oxidation.

336 **4.2 Whole-ecosystem warming increases substrate availability for methanogens**

337 Methanogenesis can be the terminal step of anaerobic decomposition, but a consortium of microbes is
338 required to break down soil organic matter to electron donor substrates that methanogens can metabolize.
339 The final step in any decomposition pathway involves the flow of electrons from organic matter (electron
340 donors) to a TEA. Under anaerobic conditions, this is accomplished by microbes that tend to specialize in
341 one TEA and compete for organic C as an electron donor (Megonigal et al., 2004). Consequently, the
342 supply of both electron donors and TEAs ~~regulates~~ the multi-step process of anaerobic
343 decomposition and thus ultimately control CH₄ emissions. **MethanogenicFor all pathways, methanogenic**
344 activity is typically limited by the supply of electron donors, including low-molecular-weight organic
345 compounds (e.g. acetate, Neubauer & Craft, 2009) and H₂, a product of organic matter fermentation. We
346 propose that whole-ecosystem warming increases the availability of previously limited C substrates
347 ~~through~~ in two pathwaysaspects (Fig. 7, mechanism 2).

348 First, warming may directly influence C availability through biochemical kinetics. Even if organic
349 inputs remained constant, warming likely accelerates fermentation of soil organic matter, ~~presumably~~
350 increasing substrate availability for methanogens. Second, the warmed plots had longer growing seasons
351 than the unheated controls (Noyce et al., 2019). This ~~increases~~ presumably increased inputs of root
352 exudates and fresh detritus, accelerating all forms of heterotrophic microbial respiration by providing

353 organic material that ~~can be broken down~~ is decomposed into acetate, H₂, low-molecular-weight organic C
354 compounds and other electron donors H₂ (Philippot et al., 2009) and stimulating CH₄ emissions from
355 warmed plots, particularly during the growing season as seen here. In 2017, we measured GPP at the
356 same time as CH₄ emissions and observed that CH₄ emissions were positively correlated with GPP and
357 that this effect increased with warming (Fig. Philippot et al., 2009), stimulating growing season CH₄
358 emissions from warmed plots. In 2017, we observed that gross primary production was positively
359 correlated with CH₄ emissions and that this effect increased with warming (Fig. S6). Prior studies have
360 also linked CH₄ production or emissions to rates of photosynthesis (Vann & Megonigal, 2003), periods of
361 active growth (Chen et al., 2017; Ward et al., 2013) (Chen et al., 2017; Ward et al., 2013), and plant
362 senescence which coincides with a pulse input of labile C from plants to soils (Bardgett et al., 2005).

363 Temperature-accelerated biochemical kinetics and increased electron-donor supply are mechanisms
364 that can increase methanogenesis without necessarily shifting methanogenic pathways. However, shifts in
365 the balance between hydrogenotrophic, acetoclastic, and methylotrophic methanogenesis pathways can be
366 expected with warming. For example, in Arctic permafrost, methylotrophic methanogenesis was found to
367 be more sensitive to warming than the other pathways (de Jong et al., 2018). Such shifts can be quantified
368 with future analyses of H₂ and low-molecular-weight organic compounds (e.g. Bridgham et al., 2013;
369 Yang et al., 2016), isotopic tracing of specific methanogenic pathways (e.g. Blaser & Conrad, 2016;
370 Conrad, 2005; Neumann et al., 2016; Whiticar, 1999) and molecular community analyses (e.g. Bridgham
371 et al., 2013; He et al., 2015; Wilson et al., 2016).

372 4.4 Whole-ecosystem warming reduces competition with sulfate reducers

373 While acetate and other low-molecular-weight organic compounds are important electron donors for
374 acetoclastic methanogenic respiration, they are also a key substrate for other microbial groups
375 including such as SO₄ reducers (Megonigal et al., 2004; Ye et al., 2014). As a result, consumption of the
376 limited acetate organic carbon supply by SO₄ reducers should (and often does) limit methanogenic

377 activity, such that terminal microbial respiration is typically dominated by SO_4 reduction in brackish
378 marshes (Sutton-Grier et al., 2011).

379 ~~We did not measure rates of SO_4 reduction in this study. Similarly, SO_4 reducers are more efficient~~
380 ~~than methanogens at competing for the H_2 required for CO_2 reduction (Kristjansson et al., 1982). We did~~
381 ~~not measure rates of SO_4 reduction in this study~~ but can use SO_4 depletion as a proxy; more SO_4 depletion
382 indicates that more SO_4 reduction has occurred. Warming generally increased SO_4 depletion, especially in
383 the plots dominated by *Schoenoplectus* (Fig. 6b). Differences in SO_4 depletion between plots is not driven
384 by SO_4 inputs because the only supply of SO_4 is the tidal flow, which is the same for all plots in each
385 community of the experiment. Instead, higher rates of SO_4 reduction are most likely driven by some
386 combination of electron donor supply and kinetics. While SO_4 reducers likely benefited from the
387 increased availability of electron donors, as described above, the kinetics of SO_4 reduction also respond
388 strongly to temperature (Weston & Joye, 2005).

389 When SO_4 concentrations drop below a threshold concentration, SO_4 reduction becomes SO_4 -limited,
390 rather than electron donor-limited (Megonigal et al., 2004). A review of the coastal wetland CH_4 literature
391 estimated this threshold at 4 mmol SO_4 (Poffenbarger et al., 2011), a value that is consistent with patterns
392 of porewater $\text{[CH}_4]$ and $\text{[SO}_4]$ at the GCReW site (Keller et al. 2009). As SO_4 and O_2 are the dominant
393 electron-accepting compounds that suppress methanogenesis in this organic soil, this drawdown then
394 releases the methanogens from substrate competition (Fig. 7, mechanism 3). Here, we show that $\text{[SO}_4]$ is
395 typically below 4 mmol in the +5.1 plots in the C_3 community and in all plots in the C_4 community (Fig.
396 6, Fig. S5). The drawdown of SO_4 may also reduce rates of anaerobic CH_4 oxidation (Hinrichs & Boetius,
397 2003). Van Hulzen et al. (1999) proposed a multi-phase system in a warming incubation experiment,
398 observing that first methanogens are out-competed for substrates by other microbes, next CH_4 production
399 increases as the supply of inhibiting TEA decreases, and finally ~~the TEA availability is~~
400 ~~reduced~~ to the point that methanogenesis is controlled only by the supply of electron donors. Warming in
401 this study decreased ~~the~~ time required for the system to pass through the first two phases (van Hulzen et
402 al., 1999). In our ~~study experiment~~, this final phase of increased methanogenic activity occurs when SO_4

403 concentrations dip below 4 mmol $\text{SO}_4 \text{ L}^{-1}$, which occurs most often in the +5.1 °C plots, especially in the
404 C₃ community. This interpretation is also supported by the long-term record of porewater chemistry from
405 an allied experiment at the site, demonstrating that porewater CH₄ concentrations increase as SO₄
406 concentrations decrease (Keller et al., 2009).

407 Methanogens may also have a competitive advantage over SO₄ reducers for electron donor
408 consumption at warmer temperatures (van Hulzen et al., 1999). Sulfate reducers and methanogens have
409 very similar K_M values for acetate, but the K_M for acetoclastic methanogenesis may decrease with
410 temperature whereas K_M values for SO₄ reducers increase with temperature (van Bodegom & Stams,
411 1999). If this is the case in our system then warming would allow methanogens to use a greater proportion
412 of the available acetate and other organic compoundssubstrates.

413 4.5 Plant traits modify warming effects on CH₄ cycling

414 The three biogeochemical mechanisms we propose to explain a warming-induced increase in CH₄
415 emissions should interact strongly with plant responses to warming. Relationships between plant
416 functional groups and CH₄ emissions have been demonstrated through field studies in other wetland
417 ecosystems such as peatlands (Bubier et al., 1995; Ward et al., 2013) (Bubier et al., 1995, Ward et al.,
418 2013) and in tidal wetland mesocosms (L. Liu et al., 2019; Martin & Moseman Valtierra, 2017; Mueller
419 et al., in press). We provide field evidence that two species with distinct plant traits — *Schoenoplectus* and
420 *Spartina* — have strikingly different effects on CH₄ emissions from brackish wetlands. *Spartina*
421 dominated communities had consistently higher CH₄ emissions under both ambient and warmed
422 conditions (Fig. 3). In most years, *Schoenoplectus* biomass was negatively correlated with CH₄ emissions,
423 while *Spartina/Distichlis* biomass was positively correlated. Vegetation effects are typically strongest
424 during the growing season, when the plants are actively altering rhizosphere biogeochemistry (F. J. W. A.

425 ~~van der Nat & Middelburg, 1998; Ward et al., 2013~~, which is consistent with our observations in this
426 ~~study~~.

427 As with warming effects, plant driven shifts in CH₄ emissions are the result of differing rates of CH₄
428 production, oxidation, transport, or a combination of these processes, but sustained differences in
429 emissions cannot be attributed only to transport, as discussed previously. Instead, the stimulation of CH₄
430 emissions is likely due to changes in the plant mediated supply of electron acceptors and electron donors.
431 In a field environment, differentiating between species specific effects and underlying environmental
432 conditions can be difficult, but mesocosm studies that control all environmental factors have also found
433 species specific effects on CH₄ cycling (e.g. (D. Liu et al., 2014). Plants can alter CH₄ cycling by adding
434 O₂ (electron acceptor) or C substrates (electron donors) to the rhizosphere, altering the redox state. We
435 propose that *Schoenoplectus* is a net oxidizer of the rhizosphere and that *Spartina* is a net reducer, and
436 thus their presence and productivity have opposing effects on CH₄ emissions (Fig. 7, mechanism 4).

437 *4.5.1 Schoenoplectus oxidizes the rhizosphere, increasing CH₄ oxidation*

438 Species vary in their capacity to support aerobic CH₄ oxidation (van der Nat & Middelburg, 1998)
439 and in tidal wetland mesocosms (Liu et al., 2019; Martin & Moseman-Valtierra, 2017; Mueller et al.,
440 2020). We provide field evidence that two species with distinct plant traits -- *Schoenoplectus* and *Spartina*
441 -- have strikingly different effects on CH₄ emissions from brackish wetlands. *Spartina*-dominated
442 communities had consistently higher CH₄ emissions under both ambient and warmed conditions (Fig. 3).
443 In most years, *Schoenoplectus* biomass was negatively correlated with CH₄ emissions, while
444 *Spartina/Distichlis* biomass was positively correlated. Vegetation effects are typically strongest during the
445 growing season, when the plants are actively altering rhizosphere biogeochemistry (van der Nat &
446 Middelburg, 1998; Ward et al., 2013), which is consistent with our observations in this study.

447 As with warming effects, plant-driven shifts in CH₄ emissions are the result of differing rates of CH₄
448 production, oxidation, transport, or a combination of these processes, but sustained differences in
449 emissions cannot be attributed only to transport, as discussed previously. Instead, the stimulation of CH₄

450 emissions is likely due to changes in the plant-mediated supply of electron acceptors and electron donors.
451 In a field environment, differentiating between species-specific effects and underlying environmental
452 conditions can be difficult, but mesocosm studies that control all environmental factors have also found
453 species-specific effects on CH₄ cycling (e.g. Liu et al., 2014). Plants can alter CH₄ cycling by adding O₂
454 (electron acceptor) or C substrates (electron donors) to the rhizosphere, altering the redox state. We
455 propose that *Schoenoplectus* is a net oxidizer of the rhizosphere and that *Spartina* is a net reducer, and
456 thus their presence and productivity have opposing effects on CH₄ emissions (Fig. 7, mechanism 4).

457 4.5.1 *Schoenoplectus* oxidizes the rhizosphere, increasing CH₄ oxidation

458 Species vary in their capacity to support aerobic CH₄ oxidation (van der Nat & Middelburg, 1998)
459 and *Schoenoplectus* appears to support higher rates of aerobic CH₄ oxidation than *Spartina* (Mueller et
460 al., *in press*).(Mueller et al., 2020). *Scirpus lacustris* is morphologically similar to *Schoenoplectus*
461 *americanus* studied here and has been demonstrated to have substantial rhizosphere rhizosphere oxidation
462 capacity, especially during the growing season (van der Nat & Middelburg, 1998)(van der Nat &
463 Middelburg, 1998). Consequently, these plants likely exert stronger control on rates of CH₄ oxidation
464 than rates of methanogenesis (van der Nat & Middelburg, 1998). We hypothesize that the relatively high
465 capacity of *Schoenoplectus* to transport O₂ held the CH₄ emissions stimulation caused by modest levels of
466 warming (+1.7 to +3.4 °C) to rates similar to under ambient conditions (Fig. 3). At high warming (+5.1
467 °C), however, *Schoenoplectus* community CH₄ emissions drastically increase (Fig. 3). We suggest that
468 this is due to the combined effects of the three mechanisms discussed previously, namely the differences
469 in the Q₁₀-values of CH₄ production and CH₄ oxidation, the increased supply of organic substrate through
470 plant productivity, and the decrease in competition for electron donors due to SO₄ depletion. Collectively,
471 when the ecosystem is warmed above current ambient conditions by 5 °C or more, enhanced stimulation
472 of CH₄ production starts to offset some of the *Schoenoplectus* oxidation effect. This also offers an
473 explanation for the positive correlation between *Schoenoplectus* biomass and CH₄ emissions observed in
474 2016 as that was the hottest of the four years in this study.

475 4.5.2 *Spartina* reduces the rhizosphere, increasing CH_4 production

476 The variability in quality and quantity of root exudates between plant functional types is well known
477 to affect microbial community composition and activity (Deyn et al., 2008). Methanogenesis responses to
478 warming in incubation studies are related to the lignin and cellulose content of the peat, which in turn
479 depends on the plant functional type from which the peat developed (Duval & Radu, 2018). Although
480 warming is likely increasing substrate availability across the whole experiment, the production ~~rate~~ of
481 labile, low-molecular-weight C substrates through fermentation ~~does not increase as rapidly as less~~
482 ~~sensitive to temperature~~ above 25 °C ~~than below this threshold~~ (Scott C Neubauer & Craft, 2009; Weston
483 & Joye, 2005). Microbes may also preferentially use root exudates as their C sources (Neubauer & Craft,
484 2009; Weston & Joye, 2005). Microorganisms may also preferentially use freshly produced (i.e. labile)
485 organic carbon compounds as electron donors (Delarue et al., 2014) (DeLaune et al., 2014) and
486 consequently warming effects on CH_4 production should be strongest in a system where ~~the plants~~ ~~rates of~~
487 ~~root exudation and turnover~~ are ~~directly releasing key C substrates most rapidly~~. We propose ~~this explains~~
488 ~~the patterns that root exudation and turnover explain the positive correlation between plant biomass and~~
489 ~~CH_4 emissions~~ that we observed in the C_4 community. Multiple years of porewater chemistry at this site
490 show that *Spartina*-dominated communities have higher DOC and dissolved CH_4 than adjacent
491 *Schoenoplectus* communities (Keller et al., 2009; Marsh et al., 2005) (Keller et al., 2009; Marsh et al.,
492 2005). Though we did not directly measure root exudation, porewater DOC is partially derived from root
493 ~~exudation~~ ~~exudates~~ and has been used as a proxy to understand the responses of root exudates to global
494 change factors (Dieleman et al., 2016; Fenner et al., 2007; Jones et al., 2009) (Dieleman et al., 2016;
495 Fenner et al., 2007; Jones et al., 2009).
496 We observed a simultaneous increase in dissolved CH_4 at the soil surface and a decrease in dissolved
497 CH_4 at depth in the warmed C_4 plots. As with the observed trends in CH_4 emissions, there are multiple
498 mechanisms that could cause a shift in porewater CH_4 concentrations. Of the four mechanisms outlined
499 above, perhaps the simplest explanation is an increase in labile C at shallow depths and a decrease in
500 deeper soil. This is consistent with DOC depth profiles from this the C_4 community in which porewater

501 DOC increases with warming in shallow samples but decreases with warming in deep samples (Fig. S7).
502 This shallowing of peak DOC concentrations could be due to a warming-induced increase in
503 evapotranspiration, leading to slower downward hydrologic transport of DOC-rich surface porewater to
504 lower depths, or a warming-induced shallowing of the root system, leading to a shift in the location of
505 root exudates.

506 In most years, *Spartina* biomass was positively correlated with CH₄ emissions, supporting our
507 hypothesis that *Spartina* favors net CH₄ production. However, in 2016 *Spartina* biomass and CH₄
508 emissions were negatively correlated. Prior work at this site has indicated that *Spartina/Distichlis* biomass
509 is more negatively affected by hot and dry growing conditions than *Schoenoplectus* (Noyce et al., 2019)
510 due in part because the *Spartina/Distichlis* (C₄) communities are less frequently inundated. The 2016
511 growing season was substantially warmer than average (Table 2) and the heating treatments were
512 initialized on 1 Jun of that year, after the annual plants had already established and may have developed
513 adaptations to ambient, rather than elevated, temperature conditions. The combination of these two effects
514 likely led to heat stress, reducing the root exudates supplied to the rhizosphere microbial community
515 (Heckathorn et al., 2013) and thus minimizing the *Spartina* stimulation effect.

516 4.6 Comparisons with prior data

517 Methane emissions have been measured at the GCReW site previously, but this study represents the most
518 comprehensive dataset collected to date, and is thus particularly useful for advancing the process-based
519 understanding needed to improve prognostic models. Overall, our flux estimates are lower than those
520 reported previously. The earliest CH₄ fluxes were measured in a single month (July) in *Schoenoplectus*-
521 dominated plots and reported to be 331 to 6883 $\mu\text{mol m}^{-2} \text{d}^{-1}$ (Dacey et al., 1994), much higher than our
522 range of 359 to 1651 $\mu\text{mol m}^{-2} \text{d}^{-1}$ for ambient temperature *Schoenoplectus* plots in July. Similarly, Marsh
523 et al. (2005) Marsh et al. (2005) reported mean growing season (May-Oct) CH₄ emissions from this site of
524 846 \pm 111 $\mu\text{mol CH}_4 \text{ m}^{-2} \text{ d}^{-1}$, whereas we measured 656 \pm 79 $\mu\text{mol CH}_4 \text{ m}^{-2} \text{ d}^{-1}$ over the same months.

525 Finally, Pastore et al. (2017) estimated average annual fluxes in their *Schoenoplectus*-dominated ambient
526 CO₂ plots as 3.1 \pm 1.7 g CH₄ m⁻² yr⁻¹, compared to our estimates of 1.6 \pm 0.3 g CH₄ m⁻² yr⁻¹ for

527 *Schoenoplectus* plots. The different estimates by these studies may be partly due to interannual variability
528 as demonstrated in our data where 2018 had substantially higher fluxes than any of the surrounding years
529 (Table S2).

530 The annual estimates reported here for ambient temperature plots trended lower than published
531 mean CH₄ emissions for mesohaline tidal marshes. Our plots ranged from 0.7 to 9.3 g CH₄ m⁻² yr⁻¹ (mean
532 = 9.3), compared to the range of 3.3 to 16.4 g CH₄ m⁻² yr⁻¹ (mean = 16.4) reported by Poffenbarger et al.
533 (2011). This difference may be explained by the fact that there was significant within-class variation in
534 the oligohaline and mesohaline salinity classes that was unexplained and their assessment was based on
535 too few data points to fully capture the variation that is expected to exist in the mesohaline class. Indeed,
536 subsequent studies have documented fluxes well below 3 g CH₄ m⁻² yr⁻¹ (Krauss & Whitbeck, 2012), and
537 even negative fluxes (Al-Haj & Fulweiler, 2020). We hypothesize that the low fluxes measured at our site
538 reflect *Schoenoplectus americanus* traits that favor CH₄ oxidation more than CH₄ production, and that the
539 high end of our range was limited by the high soil elevation (i.e. deep water table) of areas dominated by
540 *Spartina patens*, off-setting the influence of *S. patens* traits that favor CH₄ production.

541 4.7 Implications for tidal wetland carbon cycling

542 Warming accelerates rates of CH₄ emissions from brackish marshes, especially during the growing
543 season. This is driven by both direct and indirect warming effects and mediated by soil biogeochemistry,
544 but the magnitude of the warming effect is also dependent on traits of the plant species that dominate the
545 plant community. Communities dominated by *Spartina patens* increase net CH₄ emissions in response to
546 smaller increments of warming than communities dominated by *Schoenoplectus americanus*. *Spartina*-
547 dominated sites may thus have a higher likelihood of shifting from a net C sink to a net C source under
548 future warming conditions, due to this increased loss of C as CH₄. However, this effect could be mitigated
549 if these high-elevation *Spartina* marshes become dominated by *Schoenoplectus* in response to predicted
550 accelerated sea-level rise (Kirwan & Guntenspergen, 2012). In addition, *Spartina* traits are plastic and
551 influenced by factors such as soil redox conditions (Kladze & DeLaune, 1994)(Kladze & DeLaune,
552 1994), salinity (Crozier & DeLaune, 1996), and water level (Liu et al., 2019)(Liu et al., 2019), all of

553 which can be expected to change plant-mediated effects on CH₄ biogeochemistry. Further studies are
554 needed to thoroughly assess the range of environmental conditions under which *Spartina* is a net reducer
555 and *Schoenoplectus* is a net oxidizer as proposed by the present study.

556

557 **Data availability**

558 All data is available from the corresponding author upon request.

559

560 **Author contributions**

561 GLN and JPM designed the study, GLN collected and analyzed the data, and GLN and JPM wrote the
562 paper.

563

564 **Competing interests**

565 The authors declare that they have no conflict of interest.

566

567 **Acknowledgements**

568 This manuscript is based upon work supported by the U.S. Department of Energy, Office of Science,
569 Office of Biological and Environmental Research Program (DE-SC0014413 and DE-SC0019110), the
570 National Science Foundation Long-Term Research in Environmental Biology Program (DEB-0950080,
571 DEB-1457100, and DEB-1557009), and the Smithsonian Institution. Roy Rich designed the warming
572 infrastructure and maintains it with the assistance of Gary Peresta. We also thank technicians in the SERC
573 Biogeochemistry Lab for assistance with porewater collection and analysis.

574

575 **References**

576 Al-Haj, A. N., & Fulweiler, R. W. (2020). A synthesis of methane emissions from shallow vegetated
577 coastal ecosystems. *Global Change Biology*, 26(5), 2988–3005. <https://doi.org/10.1111/gcb.15046>

578 Bardgett, R. D., Bowman, W. D., Kaufmann, R., & Schmidt, S. K. (2005). A temporal approach to
579 linking aboveground and belowground ecology. *Trends in Ecology & Evolution*, 20(11), 634–641.
580 <https://doi.org/10.1016/j.tree.2005.08.005>

581 Basiliko, N., Stewart, H., Roulet, N. T., & Moore, T. R. (2012). [Do Root Exudates Enhance Peat](#)
582 [Deecomposition? Do root exudates enhance peat decomposition?](#) *Geomicrobiology Journal*, 29(4),
583 374–378. <https://doi.org/10.1080/01490451.2011.568272>

584 [Bianchi, T. S. \(2006\). *Biogeochemistry of Estuaries*. Oxford University Press.](#)

585 [Blaser, M., & Conrad, R. \(2016\). Stable carbon isotope fractionation as tracer of carbon cycling in anoxic](#)
586 [soil ecosystems. *Current Opinion in Biotechnology*, 41, 122–129.](#)
587 <https://doi.org/10.1016/j.copbio.2016.07.001>

588 Bridgham, S. D., Cadillo-Quiroz, H., Keller, J. K., & Zhuang, Q. (2013). Methane emissions from
589 wetlands: Biogeochemical, microbial, and modeling perspectives from local to global scales. *Global*
590 *Change Biology*, 19(5), 1325–1346. <https://doi.org/10.1111/gcb.12131>

591 Bridgham, S. D., Megonigal, J. P., Keller, J. K., Bliss, N. B., & Trettin, C. (2006). The carbon balance of
592 North American wetlands. *Wetlands*, 26(4), 889–916. [https://doi.org/10.1672/0277-5212\(2006\)26\[889:TCBONA\]2.0.CO;2](https://doi.org/10.1672/0277-5212(2006)26[889:TCBONA]2.0.CO;2)

593 Bubier, J. L., Moore, T. R., Bellisario, L., Comer, N. T., & Crill, P. M. (1995). Ecological controls on
594 methane emissions from a Northern Peatland Complex in the zone of discontinuous permafrost,
595 Manitoba, Canada. *Global Biogeochemical Cycles*, 9(4), 455–470.
596 <https://doi.org/10.1029/95GB02379>

597 Chen, J., Luo, Y., Xia, J., Wilcox, K. R., Cao, J., Zhou, X., Jiang, L., Niu, S., Estera, K. Y., Huang, R.,
598 Wu, F., Hu, T., Liang, J., Shi, Z., Guo, J., & Wang, R.-W. (2017). Warming [Effects](#) on
599 [Ecosystem Carbon Fluxes Are Modulated](#) [ecosystem carbon fluxes are modulated by Plant Functional](#)
600 [Types](#) [plant functional types](#). *Ecosystems*, 20(3), 515–526. <https://doi.org/10.1007/s10021-016-0035-6>

601 Christensen, T. R., Ekberg, A., Ström, L., Mastepanov, M., Panikov, N., Öquist, M., Svensson, B. H.,
602 Nykänen, H., Martikainen, P. J., & Oskarsson, H. (2003). Factors controlling large scale variations in
30

604 methane emissions from wetlands. *Geophysical Research Letters*, 30(7), 1414.

605 <https://doi.org/10.1029/2002GL016848>

606 Conrad, R. (2005). Quantification of methanogenic pathways using stable carbon isotopic signatures: A
607 review and a proposal. *Organic Geochemistry*, 36(5), 739–752.
608 <https://doi.org/10.1016/j.orggeochem.2004.09.006>

609 Conrad, R. (2020). Importance of hydrogenotrophic, aceticlastic and methylotrophic methanogenesis for
610 methane production in terrestrial, aquatic and other anoxic environments: A mini review. *Pedosphere*,
611 30(1), 25–39. [https://doi.org/10.1016/S1002-0160\(18\)60052-9](https://doi.org/10.1016/S1002-0160(18)60052-9)

612 Crozier, C. R., & DeLaune, R. D. (1996). Methane production by soils from different Louisiana marsh
613 vegetation types. *Wetlands*, 16(2), 121–126. <https://doi.org/10.1007/BF03160685>

614 Dacey, J. W. H., Drake, B. G., & Klug, M. J. (1994). Stimulation of methane emission by carbon dioxide
615 enrichment of marsh vegetation. *Nature*, 370(6484), 47–49. <https://doi.org/10.1038/370047a0>

616 de Jong, A. E. E., in 't Zandt, M. H., Meisel, O. H., Jetten, M. S. M., Dean, J. F., Rasigraf, O., & Welte,
617 C. U. (2018). Increases in temperature and nutrient availability positively affect methane-cycling
618 microorganisms in Arctic thermokarst lake sediments. *Environmental Microbiology*, 20(12), 4314–
619 4327. <https://doi.org/10.1111/1462-2920.14345>

620 Delarue, F., Gogo, S., Buttler, A., Bragazza, L., Jassey, V. E. J., Bernard, G., & Laggoun-Défarge, F.
621 (2014). Indirect effects of experimental warming on dissolved organic carbon content in subsurface
622 peat. *Journal of Soils and Sediments*, 14(11), 1800–1805. <https://doi.org/10.1007/s11368-014-0945-x>

623 Deyn, G. B. D., Cornelissen, J. H. C., & Bardgett, R. D. (2008). Plant functional traits and soil carbon
624 sequestration in contrasting biomes. *Ecology Letters*, 11(5), 516–531. [0248.2008.01164.x](https://doi.org/10.1111/j.1461-
625 0248.2008.01164.x)

626 Dieleman, C. M., Lindo, Z., McLaughlin, J. W., Craig, A. E., & Branfireun, B. A. (2016). Climate change
627 effects on peatland decomposition and porewater dissolved organic carbon biogeochemistry.
628 *Biogeochemistry*, 128(3), 385–396. <https://doi.org/10.1007/s10533-016-0214-8>

629 Ding, W., Cai, Z., & Tsuruta, H. (2005). Plant species effects on methane emissions from freshwater
630 marshes. *Atmospheric Environment*, 39(18), 3199–3207.
631 <https://doi.org/10.1016/j.atmosenv.2005.02.022>

632 Dise, N. B., Gorham, E., & Verry, E. S. (1993). Environmental factors controlling methane emissions
633 from peatlands in northern Minnesota. *Journal of Geophysical Research: Atmospheres*, 98(D6),
634 10583–10594. <https://doi.org/10.1029/93JD00160>

635 Duval, T. P., & Radu, D. D. (2018). Effect of temperature and soil organic matter quality on greenhouse-
636 gas production from temperate poor and rich fen soils. *Ecological Engineering*, 114, 66–75.
637 <https://doi.org/10.1016/j.ecoleng.2017.05.011>

638 Environmental Protection Agency. (2017). *Inventory of U.S. Greenhouse Gas Emissions and Sinks: 1990-
639 2015*. (EPA 430-P-17-001).

640 Fenner, N., Freeman, C., Lock, M. A., Harmens, H., Reynolds, B., & Sparks, T. (2007). Interactions
641 between Elevated~~elevated~~ CO₂ and Warming~~Could Amplify~~warming could amplify DOC
642 Exports~~exports~~ from Peatland~~Catchments~~peatland catchments. *Environmental Science &*
643 *Technology*, 41(9), 3146–3152. <https://doi.org/10.1021/es061765v>

644 Fey, A., & Conrad, R. (2000). Effect of temperature on carbon and electron flow and on the archaeal
645 community in methanogenic rice field soil. *Applied and Environmental Microbiology*, 66(11), 4790–
646 4797. <https://doi.org/10.1128/AEM.66.11.4790-4797.2000>

647 He, S., Malfatti, S. A., McFarland, J. W., Anderson, F. E., Pati, A., Huntemann, M., Tremblay, J., Rio, T.
648 G. del, Waldrop, M. P., Windham-Myers, L., & Tringe, S. G. (2015). Patterns in wetland microbial
649 community composition and functional gene repertoire associated with methane emissions. MBio,
650 6(3), e00066-15. https://doi.org/10.1128/mBio.00066-15

651 Heckathorn, S. A., Giri, A., Mishra, S., & Bista, D. (2013). Heat Stress and Roots. In *Climate Change*
652 *and Plant Abiotic Stress Tolerance* (pp. 109–136). John Wiley & Sons, Ltd.
653 <https://doi.org/10.1002/9783527675265.ch05>

654 Hinrichs, K.-U., & Boetius, A. (2003). The Anaerobic Oxidation of Methane: New Insights in Microbial
655 Ecology and Biogeochemistry. In G. Wefer, D. Billett, D. Hebbeln, B. B. Jørgensen, M. Schlüter, &
656 T. C. E. van Weering (Eds.), *Ocean Margin Systems* (pp. 457–477). Springer.
657 https://doi.org/10.1007/978-3-662-05127-6_28

658 [Holmquist, J. R., Windham-Myers, L., Bliss, N., Crooks, S., Morris, J. T., Megonigal, J. P., Troxler, T.,](#)
659 [Weller, D., Callaway, J., Drexler, J., Ferner, M. C., Gonnea, M. E., Kroeger, K. D., Schile-Beers, L.,](#)
660 [Woo, I., Buffington, K., Breithaupt, J., Boyd, B. M., Brown, L. N., ... Woodrey, M. \(2018\). Accuracy](#)
661 [and precision of tidal wetland soil carbon mapping in the conterminous United States. *Scientific*](#)
662 [Reports](#), 8(1), 9478. <https://doi.org/10.1038/s41598-018-26948-7>

663 Hopple, A. M., Wilson, R. M., Kolton, M., Zalman, C. A., Chanton, J. P., Kostka, J., Hanson, P. J.,
664 Keller, J. K., & Bridgman, S. D. (2020). Massive peatland carbon banks vulnerable to rising
665 temperatures. *Nature Communications*, 11(1), 2373. <https://doi.org/10.1038/s41467-020-16311-8>

666 Hosono, T., & Nouchi, I. (1997). The dependence of methane transport in rice plants on the root zone
667 temperature. *Plant and Soil*, 191(2), 233–240. <https://doi.org/10.1023/A:1004203208686>

668 Inglett, K. S., Inglett, P. W., Reddy, K. R., & Osborne, T. Z. (2012). Temperature sensitivity of
669 greenhouse gas production in wetland soils of different vegetation. *Biogeochemistry*, 108(1–3), 77–
670 90. <https://doi.org/10.1007/s10533-011-9573-3>

671 IPCC. (2013). *Limate Change 2013: The Physical Science Basis. Working Group I Contribution to the*
672 *Fifth Assessment Report of the Intergovernmental Panel on Climate Change.*
673 www.ipcc.ch/report/ar5/wg1/

674 Jones, T. G., Freeman, C., Lloyd, A., & Mills, G. (2009). Impacts of elevated atmospheric ozone on
675 peatland below-ground DOC characteristics. *Ecological Engineering*, 35(6), 971–977.
676 <https://doi.org/10.1016/j.ecoleng.2008.08.009>

677 Kayranli, B., Scholz, M., Mustafa, A., & Hedmark, Å. (2010). Carbon [Storage](#) and [Fluxes](#)
678 within [Freshwater Wetlands](#)[freshwater wetlands](#): A [Critical Review](#)[critical review](#). *Wetlands*, 30(1),
679 111–124. <https://doi.org/10.1007/s13157-009-0003-4>

680 Keller, J. K., Wolf, A. A., Weisenhorn, P. B., Drake, B. G., & Megonigal, J. P. (2009). Elevated CO₂
681 affects porewater chemistry in a brackish marsh. *Biogeochemistry*, 96(1–3), 101–117.
682 <https://doi.org/10.1007/s10533-009-9347-3>

683 Kirwan, M. L., & Guntenspergen, G. R. (2012). Feedbacks between inundation, root production, and
684 shoot growth in a rapidly submerging brackish marsh. *Journal of Ecology*, 100(3), 764–770.
685 <https://doi.org/10.1111/j.1365-2745.2012.01957.x>

686 Kludze, H. K., & DeLaune, R. D. (1994). Methane Emissions and Growth of *Spartina*
687 patens in Response to Soil Redox Intensity. *Soil Science Society of*
688 *America Journal*, 58(6), 1838–1845. <https://doi.org/10.2136/sssaj1994.03615995005800060037x>

689 Krauss, K. W., & Whitbeck, J. L. (2012). Soil greenhouse gas fluxes during wetland forest retreat along
690 the Lower Savannah River, Georgia (USA). In *Wetlands* (Vol. 32, Issue 1, p. 7381).
691 <https://doi.org/10.1007/s13157-011-0246-8>

692 Kristjansson, J. K., Schönheit, P., & Thauer, R. K. (1982). Different K_s values for hydrogen of
693 methanogenic bacteria and sulfate reducing bacteria: An explanation for the apparent inhibition of
694 methanogenesis by sulfate. Archives of Microbiology, 131(3), 278–282.
695 <https://doi.org/10.1007/BF00405893>

696 Lenzewski, N., Mueller, P., Meier, R. J., Liebsch, G., Jensen, K., & Koop-Jakobsen, K. (2018). Dynamics
697 of oxygen and carbon dioxide in rhizospheres of Lobelia dortmanna – a planar optode study of
698 belowground gas exchange between plants and sediment. *New Phytologist*, n/a-n/a.
699 <https://doi.org/10.1111/nph.14973>

700 Liu, D., Ding, W., Yuan, J., Xiang, J., & Lin, Y. (2014). Substrate and/or substrate-driven changes in the
701 abundance of methanogenic archaea cause seasonal variation of methane production potential in
702 species-specific freshwater wetlands. *Applied Microbiology and Biotechnology*, 98(10), 4711–4721.
703 <https://doi.org/10.1007/s00253-014-5571-4>

704 Liu, L., Wang, D., Chen, S., Yu, Z., Xu, Y., Li, Y., Ge, Z., & Chen, Z. (2019). Methane
705 Emissions from Estuarine Coastal Wetlands: Implications for
34

706 Global Change Effect~~global change effect~~. *Soil Science Society of America Journal*, 83(5), 1368–
707 1377. <https://doi.org/10.2136/sssaj2018.12.0472>

708 Lu, M., Caplan, J. S., Bakker, J. D., Langley, J. A., Mozdzer, T. J., Drake, B. G., & Megonigal, J. P.
709 (2016). Allometry data and equations for coastal marsh plants. *Ecology*, 97(12), 3554–3554.
710 <https://doi.org/10.1002/ecy.1600>

711 Marsh, A. S., Rasse, D. P., Drake, B. G., & Patrick Megonigal, J. (2005). Effect of elevated CO₂ on
712 carbon pools and fluxes in a brackish marsh. *Estuaries*, 28(5), 694–704.
713 <https://doi.org/10.1007/BF02732908>

714 Martin, R. M., & Moseman-Valtierra, S. (2017). Different short-term responses of greenhouse gas fluxes
715 from salt marsh mesocosms to simulated global change drivers. *Hydrobiologia*, 802(1), 71–83.
716 <https://doi.org/10.1007/s10750-017-3240-1>

717 Mcleod, E., Chmura, G. L., Bouillon, S., Salm, R., Björk, M., Duarte, C. M., Lovelock, C. E.,
718 Schlesinger, W. H., & Silliman, B. R. (2011). A blueprint for blue carbon: Toward an improved
719 understanding of the role of vegetated coastal habitats in sequestering CO₂. *Frontiers in Ecology and
720 the Environment*, 9(10), 552–560. <https://doi.org/10.1890/110004>

721 Megonigal, J. P., Whalen, S. C., Tissue, D. T., Bovard, B. D., Allen, A. S., & Albert, D. B. (1999). A
722 ~~Plant-Soil-Atmosphere Microcosm~~^{plant-soil-atmosphere microcosm} for ~~Tracing Radioisotope~~^{tracing}
723 ~~radiocarbon~~ from ~~Photosynthesis~~^{photosynthesis} through ~~Methanogenesis~~^{methanogenesis}. *Soil
724 Science Society of America Journal*, 63(3), 665–671.
725 <https://doi.org/10.2136/sssaj1999.03615995006300030033x>

726 Megonigal, J. ~~Patrick, Chapman, S., Crooks, S., Dijkstra, P., Kirwan, M., & Langley, A.~~ (2016). 3.4
727 ~~Impacts and effects of ocean warming on tidal marsh and tidal freshwater forest ecosystems. In~~
728 ~~D. Laffoley & J. M. Baxter (Eds.), Explaining Ocean Warming: Causes, scale, effects, and~~
729 ~~consequences. IUCN.~~

730 Megonigal, J., Patrick, Hines, M. E., & Visscher, P. T. (2004). Anaerobic metabolism: Linkages to trace
731 gases and aerobic processes. In W. H. Schlesinger (Ed.), *Biogeochemistry* (pp. 317–424). Elsevier-
732 Pergamon.

733 Megonigal, J. Patrick, & Schlesinger, William. H. (2002). Methane-limited methanotrophy in tidal
734 freshwater swamps. *Global Biogeochemical Cycles*, 16(4), 1088.
735 <https://doi.org/10.1029/2001GB001594>

736 Moor, H., Rydin, H., Hylander, K., Nilsson, M. B., Lindborg, R., & Norberg, J. (2017). Towards a trait-
737 based ecology of wetland vegetation. *Journal of Ecology*, 105(6), 1623–1635.
738 <https://doi.org/10.1111/1365-2745.12734>

739 Mueller, P., Jensen, K., & Megonigal, J. P. (2016). Plants mediate soil organic matter decomposition in
740 response to sea level rise. *Global Change Biology*, 22(1), 404–414. <https://doi.org/10.1111/gcb.13082>

741 Mueller, P., Mozdzer, T. J., Langley, J. A., Aoki, L. R., Noyce, G. L., & Megonigal, J. P. ([in press 2020](#)).
742 Plants determine methane response to sea level rise. *Nature Communications*.
743 <https://doi.org/10.1038/s41467-020-18763-4>

744 Neubauer, S. C., Emerson, D., & Megonigal, J. P. (2008). Microbial oxidation and reduction of Iron in
745 the root zone and influences on metal mobility. In *Biophysico-Chemical Processes of Heavy Metals*
746 and Metalloids in Soil Environments (pp. 339–371). John Wiley & Sons, Ltd.
747 <https://doi.org/10.1002/9780470175484.ch9>

748 Neubauer, Scott C., & Craft, C. B. (2009). Chapter 23 Global Change and Tidal Freshwater Wetlands:
749 Scenarios and Impacts. In A. Barendregt, D. Whigham, & A. Baldwin (Eds.), *Tidal Freshwater*
750 *Wetlands* (pp. 253–310). Margraf Publishers.

751 Neubauer, Scott C., & Megonigal, J. P. (2015). Moving beyond global warming potentials to quantify the
752 climatic role of ecosystems. *Ecosystems*, 18(6), 1000–1013. <https://doi.org/10.1007/s10021-015-9879-4>

754 Neumann, R. B., Blazewicz, S. J., Conaway, C. H., Turetsky, M. R., & Waldrop, M. P. (2016). Modeling
755 [CH₄ and CO₂ cycling using porewater stable isotopes in a thermokarst bog in Interior Alaska: Results](#)
36

756 from three conceptual reaction networks. *Biogeochemistry*, 127(1), 57–87.

757 <https://doi.org/10.1007/s10533-015-0168-2>

758 Noyce, G. L., Kirwan, M. L., Rich, R. L., & Megonigal, J. P. (2019). Asynchronous nitrogen supply and
759 demand produce non-linear plant allocation responses to warming and elevated CO₂. *Proceedings of*
760 *the National Academy of Sciences*.

761 Oremland, R. S., Marsh, L. M., & Polcin, S. (1982). Methane production and simultaneous sulphate
762 reduction in anoxic, salt marsh sediments. *Nature*, 296(5853), 143–145.

763 <https://doi.org/10.1038/296143a0>

764 Pastore, M. A., Megonigal, J. P., & Langley, J. A. (2017). Elevated CO₂ and nitrogen addition accelerate
765 net carbon gain in a brackish marsh. *Biogeochemistry*, 133(1), 73–87. <https://doi.org/10.1007/s10533-017-0312-2>

766 Pendleton, L., Donato, D. C., Murray, B. C., Crooks, S., Jenkins, W. A., Sifleet, S., Craft, C., Fourqurean,
767 J. W., Kauffman, J. B., Marbà, N., Megonigal, P., Pidgeon, E., Herr, D., Gordon, D., & Baldera, A.
768 (2012). Estimating global “blue carbon” emissions from conversion and degradation of vegetated
769 coastal ecosystems. *PLOS ONE*, 7(9), e43542. <https://doi.org/10.1371/journal.pone.0043542>

770 Philippot, L., Hallin, S., Börjesson, G., & Baggs, E. M. (2009). Biochemical cycling in the rhizosphere
771 having an impact on global change. *Plant and Soil*, 321(1), 61–81. <https://doi.org/10.1007/s11104-008-9796-9>

772 Poffenbarger, H. J., Needelman, B. A., & Megonigal, J. P. (2011). Salinity influence on methane
773 emissions from tidal marshes. *Wetlands*, 31(5), 831–842. <https://doi.org/10.1007/s13157-011-0197-0>

774 Rich, R. L., Stefanski, A., Montgomery, R. A., Hobbie, S. E., Kimball, B. A., & Reich, P. B. (2015).
775 Design and performance of combined infrared canopy and belowground warming in the B4WarmED
776 (Boreal Forest Warming at an Ecotone in Danger) experiment. *Global Change Biology*, 21(6), 2334–
777 2348. <https://doi.org/10.1111/gcb.12855>

780 Robroek, B. J. M., Albrecht, R. J. H., Hamard, S., Pulgarin, A., Bragazza, L., Buttler, A., & Jassey, V. E.
781 (2016). Peatland vascular plant functional types affect dissolved organic matter chemistry. *Plant and*
782 *Soil*, 407(1), 135–143. <https://doi.org/10.1007/s11104-015-2710-3>

783 Roden, E. E., & Wetzel, R. G. (1996). Organic carbon oxidation and suppression of methane production
784 by microbial Fe(III) oxide reduction in vegetated and unvegetated freshwater wetland sediments.
785 Limnology and Oceanography, 41(8), 1733–1748. <https://doi.org/10.4319/lo.1996.41.8.1733>

786 Saunois, M., Bousquet, P., Poulter, B., Peregon, A., Ciais, P., Canadell, J. G., Dlugokencky, E. J., Etiöpe,
787 G., Bastviken, D., Houweling, S., Janssens-Maenhout, G., Tubiello, F. N., Castaldi, S., Jackson, R.
788 B., Alexe, M., Arora, V. K., Beerling, D. J., Bergamaschi, P., Blake, D. R., ... Peng, S. (2016). The
789 global methane budget 2000–2012. *Earth System Science Data*, 8(2), 697–751.
790 <http://dx.doi.org/10.5194/essd-8-697-2016>

791 Schlesinger, W. H., & Bernhardt, E. S. (2020). Biogeochemistry: An Analysis of Global Change (4th ed.).
792 Academic Press.

793 Segers, R. (1998). Methane production and methane consumption: A review of processes underlying
794 wetland methane fluxes. *Biogeochemistry*, 41(1), 23–51. <https://doi.org/10.1023/A:1005929032764>

795 Sih, D., Inglett, P. W., Gerber, S., & Inglett, K. S. (2017). Rate of warming affects temperature
796 sensitivity of anaerobic peat decomposition and greenhouse gas production. *Global Change Biology*,
797 24(1), e259–e274. <https://doi.org/10.1111/gcb.13839>

798 Sorrell, B. K., Brix, H., Schierup, H.-H., & Lorenzen, B. (1997). Die-back of *Phragmites australis*:
799 Influence on the distribution and rate of sediment methanogenesis. *Biogeochemistry*, 36(2), 173–188.
800 <https://doi.org/10.1023/A:1005761609386>

801 Stanley, E. H., & Ward, A. K. (2010). Effects of Vascular Plants on Seasonal Pore Water
802 Carbon Dynamics in a Lotic Wetland. *Wetlands*,
803 30(5), 889–900. <https://doi.org/10.1007/s13157-010-0087-x>

804 Sutton-Grier, Ariana. E., Keller, J. K., Koch, R., Gilmour, C., & Megonigal, J. P. (2011). Electron donors
805 and acceptors influence anaerobic soil organic matter mineralization in tidal marshes. *Soil Biology
806 and Biochemistry*, 43(7), 1576–1583. <https://doi.org/10.1016/j.soilbio.2011.04.008>

807 van Bodegom, P. M., & Stams, A. J. M. (1999). Effects of alternative electron acceptors and temperature
808 on methanogenesis in rice paddy soils. *Chemosphere*, 39(2), 167–182. [https://doi.org/10.1016/S0045-6535\(99\)00101-0](https://doi.org/10.1016/S0045-
809 6535(99)00101-0)

810 van der Nat, F.-J., & Middelburg, J. J. ([19981998a](#)). Effects of two common macrophytes on methane
811 dynamics in freshwater sediments. *Biogeochemistry*, 43(1), 79–104.
812 <https://doi.org/10.1023/A:1006076527187>

813 van der Nat, F.-J. W. A., & Middelburg, J. J. ([19981998b](#)). Seasonal variation in methane oxidation by
814 the rhizosphere of *Phragmites australis* and *Scirpus lacustris*. *Aquatic Botany*, 61(2), 95–110.
815 [https://doi.org/10.1016/S0304-3770\(98\)00072-2](https://doi.org/10.1016/S0304-3770(98)00072-2)

816 van Hulzen, J. B., Segers, R., van Bodegom, P. M., & Leffelaar, P. A. (1999). Temperature effects on soil
817 methane production: An explanation for observed variability. *Soil Biology and Biochemistry*, 31(14),
818 1919–1929. [https://doi.org/10.1016/S0038-0717\(99\)00109-1](https://doi.org/10.1016/S0038-0717(99)00109-1)

819 Vann, C. D., & Megonigal, J. P. (2003). Elevated CO₂ and water depth regulation of methane emissions:
820 Comparison of woody and non-woody wetland plant species. *Biogeochemistry*, 63(2), 117–134.
821 <https://doi.org/10.1023/A:1023397032331>

822 Waldo, N. B., Hunt, B. K., Fadely, E. C., Moran, J. J., & Neumann, R. B. (2019). Plant root exudates
823 increase methane emissions through direct and indirect pathways. *Biogeochemistry*, 145(1), 213–234.
824 <https://doi.org/10.1007/s10533-019-00600-6>

825 Ward, S. E., Ostle, N. J., Oakley, S., Quirk, H., Henrys, P. A., & Bardgett, R. D. (2013). Warming effects
826 on greenhouse gas fluxes in peatlands are modulated by vegetation composition. *Ecology Letters*,
827 16(10), 1285–1293. <https://doi.org/10.1111/ele.12167>

828 Wassmann, R., Alberto, M. C., Tirol-Padre, A., Hoang, N. T., Romasanta, R., Centeno, C. A., & Sander,
829 B. O. (2018). Increasing sensitivity of methane emission measurements in rice through deployment of
39

830 ‘closed chambers’ at nighttime. *PLOS ONE*, 13(2), e0191352.

831 <https://doi.org/10.1371/journal.pone.0191352>

832 [Weiss, J. V., Emerson, D., & Megonigal, J. P. \(2004\). Geochemical control of microbial Fe\(III\) reduction potential in wetlands: Comparison of the rhizosphere to non-rhizosphere soil. *FEMS Microbiology Ecology*, 48\(1\), 89–100. https://doi.org/10.1016/j.femsec.2003.12.014](#)

833 [Ecology, 48\(1\), 89–100. https://doi.org/10.1016/j.femsec.2003.12.014](#)

834 [Weiss, J. V., Emerson, D., & Megonigal, J. P. \(2004\). Geochemical control of microbial Fe\(III\) reduction potential in wetlands: Comparison of the rhizosphere to non-rhizosphere soil. *FEMS Microbiology Ecology*, 48\(1\), 89–100. https://doi.org/10.1016/j.femsec.2003.12.014](#)

835 Weston, N. B., & Joye, S. B. (2005). Temperature-driven decoupling of key phases of organic matter

836 degradation in marine sediments. *Proceedings of the National Academy of Sciences of the United*

837 *States of America*, 102(47), 17036–17040. <https://doi.org/10.1073/pnas.0508798102>

838 [Whiticar, M. J. \(1999\). Carbon and hydrogen isotope systematics of bacterial formation and oxidation of](#)

839 [methane. *Chemical Geology*, 161\(1\), 291–314. https://doi.org/10.1016/S0009-2541\(99\)00092-3](#)

840 Wilson, R. M., Hopple, A. M., Tfaily, M. M., Sebestyen, S. D., Schadt, C. W., Pfeifer-Meister, L.,

841 Medvedeff, C., McFarlane, K. J., Kostka, J. E., Kolton, M., Kolka, R. K., Kluber, L. A., Keller, J. K.,

842 Guilderson, T. P., Griffiths, N. A., Chanton, J. P., Bridgman, S. D., & Hanson, P. J. (2016). Stability

843 of peatland carbon to rising temperatures. *Nature Communications*, 7, ncomms13723.

844 <https://doi.org/10.1038/ncomms13723>

845 Yang, P., Wang, M. H., Lai, D. Y. F., Chun, K. P., Huang, J. F., Wan, S. A., Bastviken, D., & Tong, C.

846 (2019). Methane dynamics in an estuarine brackish *Cyperus malaccensis* marsh: Production and

847 porewater concentration in soils, and net emissions to the atmosphere over five years. *Geoderma*,

848 337, 132–142. <https://doi.org/10.1016/j.geoderma.2018.09.019>

849 [Yang, Z., Wullschleger, S. D., Liang, L., Graham, D. E., & Gu, B. \(2016\). Effects of warming on the](#)

850 [degradation and production of low-molecular-weight labile organic carbon in an Arctic tundra soil.](#)

851 [*Soil Biology and Biochemistry*, 95, 202–211. https://doi.org/10.1016/j.soilbio.2015.12.022](#)

852 Ye, R., Jin, Q., Bohannan, B., Keller, J. K., & Bridgman, S. D. (2014). Homoacetogenesis: A potentially

853 underappreciated carbon pathway in peatlands. *Soil Biology and Biochemistry*, 68(Supplement C),

854 385–391. <https://doi.org/10.1016/j.soilbio.2013.10.020>

855 Yvon-Durocher, G., Allen, A. P., Bastviken, D., Conrad, R., Gudasz, C., St-Pierre, A., Thanh-Duc, N., &

856 del Giorgio, P. A. (2014). Methane fluxes show consistent temperature dependence across
857 microbial to ecosystem scales. *Nature*, 507(7493), 488–491. <https://doi.org/10.1038/nature13164>
858
859